

Deconfinement and Percolation¹

Helmut Satz

Fakultät für Physik, Universität Bielefeld
D-33501 Bielefeld, Germany

Abstract:

Using percolation theory, we derive a conceptual definition of deconfinement in terms of cluster formation. The result is readily applicable to infinite volume equilibrium matter as well as to finite size pre-equilibrium systems in nuclear collisions.

1. Introduction

Quantum chromodynamics predicts that strongly interacting matter will undergo a transition from a low density medium consisting of colour-neutral hadrons to a plasma of deconfined coloured quarks and gluons at high densities. This transition has been confirmed and studied in detail in finite temperature lattice QCD at zero baryon number density; nevertheless, even there it can so far be formulated concisely only in the limits of infinite and of vanishing quark mass.

Infinite quark mass leads to pure colour $SU(N)$ gauge theory. Here the Polyakov loop $L(T)$ provides an order parameter suitable to define the confinement-deconfinement phase transition, driven by the underlying center $Z_N \subset SU(N)$ symmetry of the Lagrangian. Confined states share this symmetry, but it is spontaneously broken in the deconfined phase. For QCD with quarks of mass $m_q < \infty$, the symmetry is broken explicitly in the Lagrangian.

In the limit of vanishing quark mass, the Lagrangian becomes invariant under chiral transformations. Now the quark condensate $\langle \psi \bar{\psi} \rangle(T)$ constitutes an order parameter, distinguishing the hadronic phase of spontaneously broken chiral symmetry from the quark-gluon plasma, in which this symmetry is restored. In other words, in the confined phase the massless quarks ‘dress’ themselves to become massive constituent quarks, while in the deconfined phase the massless current quarks of the Lagrangian are recovered. Here as well, the introduction of a finite quark mass m_q explicitly breaks the relevant symmetry of the Lagrangian.

The real world lies between these two limits, and there the nature of the transition is less clear (Fig. 1). The aim of the present paper is to study this region of broken

¹Talk given at the International Symposium *QCD at Finite Baryon Density*, April 27 - 30, 1998, Bielefeld, Germany; *Proceedings* to appear in Nuclear Physics A.

symmetries and to look for a more general description of deconfinement which would be applicable there as well. Conceptually, the transition from hadronic matter to quark-gluon plasma seems rather transparent, no matter what the quark mass is. Once the density of constituents becomes so high that several hadrons have considerable overlap, it no longer makes sense to partition the underlying quarks into colour-neutral bound states. Instead, there appear clusters much larger than hadrons, within which colour is not confined. This suggests that deconfinement is related to cluster formation, and since that is the central topic of percolation theory, possible connections between percolation and deconfinement were discussed already quite some time ago on a rather qualitative level [1, 2]. In the meantime, however, the interrelation of geometric cluster percolation and critical behaviour of thermal systems has become much better understood [3], and we want to apply this understanding to clarify the nature of deconfinement.

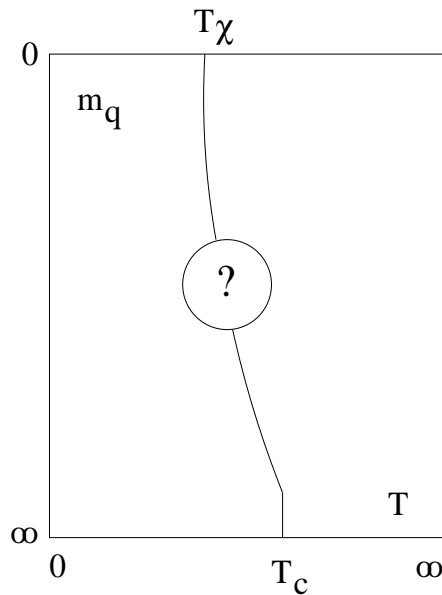


Figure 1: Critical behaviour in finite temperature QCD.

In section 2, we shall recall some aspects concerning the relation between deconfinement and chiral symmetry restoration. The main results of percolation theory for lattice systems will be summarized in section 3 and extended to continuum percolation in section 4. This will then provide the basis for the study of percolation in finite temperature and finite density QCD in section 5. Finally, in section 6, we shall consider applications to deconfinement in nuclear collisions.

2. Critical Behaviour in Finite Temperature QCD

We want to consider here in particular the role of the ‘bare’ quark mass m_q in the Lagrangian

$$\mathcal{L} = -\frac{1}{4}F_{\mu\nu}^a F_a^{\mu\nu} - \bar{\psi}_\alpha (i\gamma^\mu \partial_\mu - g\gamma^\mu A_\mu)^{\alpha\beta} \psi_\beta - m_q \bar{\psi}_\alpha \psi_\alpha \quad (1)$$

for the critical behaviour of statistical QCD. From the point of view of pure gauge theory, the introduction of m_q breaks explicitly the center Z_N symmetry of the Lagrangian and thus is like turning on an external magnetic field $H \sim 1/m_q$ in the corresponding Z_N spin theory; for infinite quark mass, we recover the thermodynamics of pure gauge theory, just as $H = 0$ leads back to the Z_N -symmetric spin system. For sufficiently small quark masses, one might thus expect a smooth temperature variation of the Polyakov loop [4], similar to the magnetization pattern of spins in a strong external field. However, such a behaviour is not observed; even for quark masses approaching the chiral limit, the Polyakov loop

$$L(T, m_q) \sim \exp\{-V(m_q)/T\} \quad (2)$$

varies very rapidly at those ‘critical’ temperatures at which energy density and chiral condensate vary strongly; here $V(m_q)$ denotes the interquark potential in the limit of large separation. The reason for this persistence of an ‘almost’ critical behaviour of $L(T, m_q)$ in T seems evident: the spontaneous breaking of the chiral symmetry for $m_q = 0$ produces an effective ‘constituent’ quark mass $M_q \simeq M_h/2$, equal to about half the mass M_h of the basic (non-Goldstone) meson. For $m_q \neq 0$, chiral symmetry is explicitly broken and $M_q(m_q)$ thus varies with m_q in the form shown in Fig. 2. Equivalently, the potential string breaks in the large distance limit not for $2m_q$, but rather for $M_h \simeq 2M_q$, so that even for $m_q \rightarrow 0$, a finite energy is still required for string breaking. It is M_q^{-1} , not the inverse bare quark mass m_q^{-1} , which acts as external field, and hence this field always remains quite weak. The range of variation of $L(T, m_q)$ thus lies between the singular pure gauge form $L(T, m_q = \infty)$ and a limiting form $L(T, m_q = 0)$ which still varies strongly with T (Fig. 3).

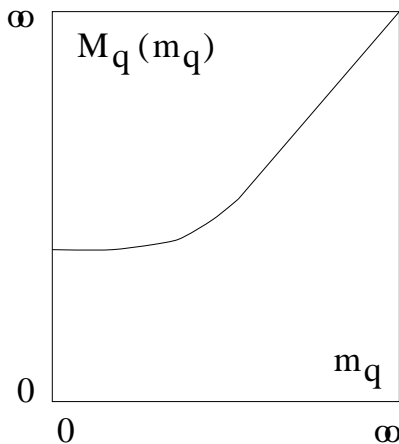


Figure 2: Variation of the constituent quark mass with bare quark mass.

The thermal pattern of $L(T, m_q)$ should be contrasted to that of the chiral condensate $\langle\psi\bar{\psi}\rangle(T, m_q)$. For $m_q = 0$, the spontaneous breaking of the chiral symmetry at low temperatures disappears when $T = T_\chi$, and from there on chiral symmetry is restored. The introduction of a non-vanishing bare quark mass m_q explicitly breaks chiral symmetry, so that here m_q (and not its inverse) acts like an external field in the corresponding $O(4)$ spin system [5]; only for $m_q = 0$ is there genuine spontaneous symmetry breaking,

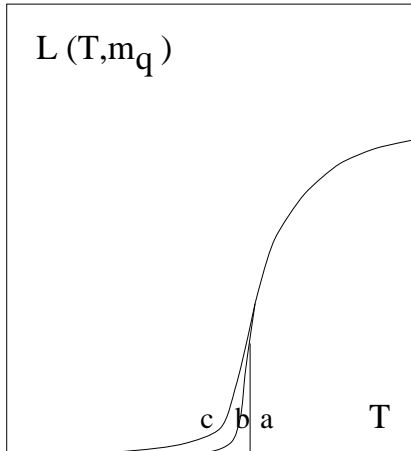


Figure 3: The temperature dependence of the Polyakov loop (a) for pure gauge theory ($m_q \rightarrow \infty$), (b) for QCD with light quarks ($0 < m_q < \infty$), and (c) in the chiral limit ($m_q = 0$).

and when m_q becomes large, the temperature variation of $\langle \psi \bar{\psi} \rangle(T, m_q)$ is washed out completely.

The ‘transition’ line between $m_q = \infty$ and $m_q = 0$ in Fig. 1 can thus be characterized as follows: the singular behaviour of $L(m_q = \infty)$ changes into an ‘almost’ singular behaviour as the quark mass becomes finite, with $L(M_q[m_q = 0])$ as the chiral limit. Any (spontaneous or explicit) breaking of chiral symmetry assures that $M_q \neq 0$ and hence limits the strength of the effective external field. The associated ‘almost’ singular behaviour of thermal observables such as entropy or energy density is thus related to deconfinement as far as the overall variation is concerned; the chiral features determine how ‘smooth’ this variation can become, and explicit or spontaneous chiral symmetry breaking keeps it always very pronounced. – While these considerations provide a reason why the deconfinement transition, as defined by the behaviour of the Polyakov loop, ‘almost’ persists in the chiral limit, they do not explain why deconfinement and chiral symmetry restoration effectively coincide at zero baryon number density; all arguments appear to remain valid if chiral symmetry were restored above deconfinement.

We now turn to percolation theory, with the aim of obtaining a characterization of deconfinement which remains valid for all values of the quark mass m_q .

3. Percolation and the Ising Model

For simplicity, consider a two-dimensional square lattice of linear size L ; we randomly place identical objects on N of the L^2 lattice sites. With increasing N , adjacent occupied sites will begin to form growing clusters or islands the sea of empty sites. Define n_p to be the lowest value of the density $n = N/L^2$ for which the origin belongs on the average (i.e., calculated by averaging over many randomly generated configurations) to a cluster reaching the edge of the lattice. In the limit of infinite lattice size, we then have

$$P(n) \sim \left(1 - \frac{n_p}{n}\right)^{\beta_p}, \quad n \geq n_p, \quad (3)$$

for n approaching n_p from above, where $P(n)$ denotes the probability that the origin belongs to an infinite cluster. Since $P(n) = 0$ for all $n \leq n_p$ and non-zero for all $n > n_p$, it constitutes an order parameter for percolation: $\beta_p = 5/36$ is the critical exponent which governs the vanishing of $P(n)$ at $n = n_p$ in two dimensions; in three dimensions, it becomes $\beta = 0.41$ [6].

For $n < n_p$, a quantity of particular interest is the ‘mean’ cluster size $S(n)$, defined as the average size (the number of connected occupied sites) of a cluster containing the origin of the lattice. As n approaches n_p from below, $S(n)$ diverges at the percolation point as

$$s_{\text{cl}}(n) \sim (n_p - n)^{-\gamma_p}, \quad n \leq n_p \quad (4)$$

with $\gamma_p = 43/18$ (1.80) as the $d = 2$ (3) critical exponent for the divergence.

Instead of the site percolation just described, a random placement of bonds on the lines between adjacent sites leads to bond percolation, with the same critical exponents. Clusters now consist of regions of connected bond lines. While the critical behaviour is universal, the value of the percolation threshold n_p depends on the type of percolation considered; on a two-dimensional square lattice, it is 0.5 for bond and 0.59 for site percolation [6].

We now turn to the Ising model, defined by the Hamiltonian

$$\mathcal{H}_I = -J \sum_{i,j} s_i s_j - H \sum_i s_i, \quad s_i = \pm 1, \quad (5)$$

where the first sum runs only over nearest neighbours on the lattice, with J denoting the exchange energy between spins and H an external field. For $H = 0$, the Hamiltonian (3) has a global Z_2 invariance ($s_i \rightarrow -s_i \forall i$), and the magnetization $m = \langle s \rangle$ probes whether this invariance is spontaneously broken. As is well-known, such spontaneous symmetry breaking occurs below the Curie point T_c , with

$$m(T, H = 0) \sim \left(1 - \frac{T_c}{T}\right)^{\beta_m} \quad (6)$$

governing the vanishing of $m(T, H = 0)$ as $T \rightarrow T_c$ from below. The well-known Onsager solution gives with $\beta_m = 0.125$ for $d = 2$ a 10 % smaller value than the $\beta_p = 5/36 \simeq 0.139$ found for the percolation exponent.

Since the Ising model also produces clusters on the lattice, consisting of connected regions of aligned up or down spins, the relation between its thermal critical behaviour at T_c and the onset of geometric percolation is an obvious question which has been studied extensively in recent years. Two important distinctions have emerged: the nature of what is defined as a cluster [7], and the behaviour of clusters in a non-vanishing external field [8, 9].

The geometric clusters considered in percolation theory consist simply of connected regions of spins pointing in the same direction. In the Ising model, there is a thermal correlation between spins on different sites; this vanishes for $T \rightarrow \infty$. Correlated regions in the Ising model (we follow the usual notation and call them ‘droplets’, to distinguish

them from geometric clusters) thus disappear in the high temperature limit. In contrast, the geometric clusters never vanish, since the probability for a finite number of adjacent aligned spins always remains finite; it increases with dimension because the number of neighbours does. Hence from the point of view of percolation, there are more and bigger clusters than there are Ising droplets. As an immediate consequence, percolation occurs in general before the onset of spontaneous magnetization.

If percolation is to provide the given thermal critical behaviour, the definition of cluster has to be changed such that the modified percolation clusters coincide with the correlated Ising droplets [7]. This is achieved by assigning to some pairs of adjacent aligned spins in a geometric cluster an additional bond correlation, randomly distributed with the density

$$n_b = 1 - \epsilon^{-2J/kT}, \quad (7)$$

where $[-2J/kT]$ just corresponds to the energy required for flipping an aligned into an opposing spin. The modified percolation clusters then consist of aligned spins which are bond connected. Only for $T = 0$ are all aligned spins bonded; for $T > 0$, some aligned spins in a purely geometric cluster are not bonded and hence do not belong to the modified cluster or droplet. This effectively reduces the size of a given geometric cluster or even cuts it into several modified clusters. For $T \rightarrow \infty$, $n_b \rightarrow 0$, so that the geometric clusters still in existence there are not counted as droplets, solving the problem mentioned in the previous paragraph.

With such a superposition of site and bond percolation ('s/b'), full agreement between percolation and thermal critical behaviour of the Ising model is achieved. An infinite percolation cluster is now formed for the first time at T_c , the cluster size coincides with that of the correlated regions in the Ising model, and numerical simulations show that the effective critical exponents for the new $P_{s/b}(n)$ or $S_{s/b}(n)$ become those of the Ising model.

However, for $H \neq 0$, Ising model and percolation theory results do not coincide, neither for purely geometric nor for site/bond defined percolation clusters. The Ising model for $H \neq 0$ does not lead to any singularity as function of T and hence does not show any critical behaviour [10]; the Z_2 symmetry responsible for the onset of spontaneous magnetization is now always broken and $m(T, H \neq 0) \neq 0$ for all T . On the other hand, the size of connected regions of aligned and bonded spins increases with decreasing temperature, and above some critical temperature it diverges. Hence percolation will occur for any value of H . At $H = \infty$, all spins are aligned, leaving the bonds as the relevant variables; the system thus percolates at the critical density for bond percolation, which is 1/2 in two and 0.249 in three dimensions, for square and cubic lattices, respectively. From Eq. (6), this corresponds to temperatures $kT_b/J = 2.89$ and 6.99 in two and three dimensions, to be compared to the Curie temperatures $kT_c/J = 2.27$ and 4.51, respectively. The corresponding values at finite H lie between T_c at $H = 0$ and T_b at $H = \infty$ and define the so-called Kertész line [3, 8]; see Fig. 4. What happens at this line in terms of dynamics?

Since the Ising model does not lead to singular behaviour in T for $H \neq 0$, in this case even the modified percolation picture does not agree with the Ising result. The reason for this is physically quite evident. At sufficiently high temperatures, only finite size

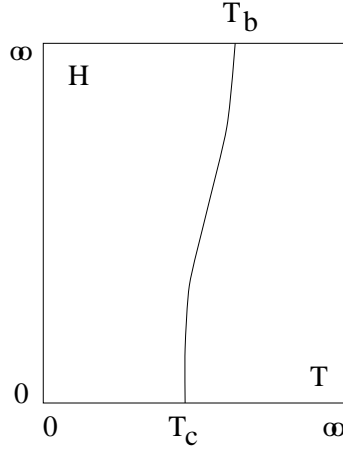


Figure 4: The Kertész line, defining the percolation temperature in the Ising model as function of the external field H ; T_c denotes the Curie temperature, T_b the pure bond percolation temperature.

s/b clusters exist, so that the percolation probability vanishes; at low temperatures, on the other hand, the s/b cluster size diverges, and hence $P(n)$ remains as genuine order parameter. The existence of a non-vanishing external field, however, partially aligns in its direction the spins of the different disconnected finite size clusters at high temperature [9], so that the overall magnetization never vanishes. As a result, the critical behaviour due to percolation persists, while that related to the thermal magnetization pattern disappears.

As is well-known, the Ising model can be reformulated as a lattice gas, where its critical behaviour describes in a rudimentary way the vapour-liquid transition. The non-singular behaviour for $H \neq 0$ then translates into a continuous cross-over from gas to liquid for sufficiently high pressure; the two phases are assumed to become indistinguishable in the relevant pressure-temperature regime. However, the percolation effect discussed in the previous paragraph seems to contradict the established credo that ‘nothing happens above the critical point’. It is observed [8, 11] that for temperatures below the Kertész line, Ising droplets have a finite surface tension; this vanishes along the Kertész line, and on its high temperature side, the droplet energy becomes proportional to their bulk energy. Note that such a behaviour does not contradict the non-singular thermodynamic behaviour of the model, since the variable that changes along the Kertész line, the surface tension of droplets, is not expressible in terms of thermodynamic observables.

In the same vein, we note another illustration of the relation between percolation and thermal critical behaviour. Consider bond percolation in the two-dimensional Ising model and imagine that current can flow between two or more bonded sites. In this case, conductivity sets in at the percolation point, independent of the thermal critical behaviour of the Ising model; the system is non-conducting below the percolation point and conducting above it. This remains true also in s/b percolation and is independent of whether clusters are partially aligned by an external field. In other words, we have two independent critical phenomena, the onset of conductivity and the critical behaviour of Ising thermodynamics. This suggests a possible framework for a general characterization

of deconfinement. Before addressing this, however, we want to point out some aspects encountered in the extension of percolation to continuum systems [6].

4. Continuum Percolation

We start again in two dimensions and consider the distribution of discs of radius r over some plane area, allowing overlap; as example, we take a circle of radius $R \gg r$ (see Fig. 5). The average cluster size s_{cl} and density n_{cl} (number of discs per cluster) is determined also here by averaging clusters containing the origin over many randomly generated configurations. These quantities are studied as function of the overall density n , i.e., the number of discs per circle πR^2 . In the limit $R \rightarrow \infty$, the percolation probability $P(n)$ and the divergence of the cluster size $S(n)$ are then given by Eqs. (3) and (4), with the same critical exponents; the same remains true for the corresponding three-dimensional case, with overlapping spheres instead of discs.

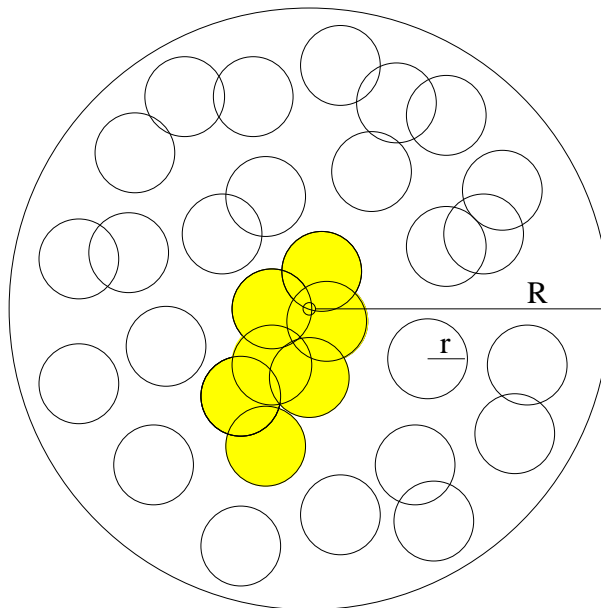


Figure 5: Two-dimensional continuum clustering.

In the continuum, the percolation threshold becomes [6, 12]

$$n_p \simeq \frac{1.18}{\pi r^2} \quad (8)$$

for $d = 2$ and

$$n_p \simeq \frac{0.34}{(4\pi/3)r^3} \quad (9)$$

for $d = 3$. In both cases, there is considerable overlap, and at the percolation point, the fraction of the area (volume) covered by discs (spheres) is $1 - \exp(-\eta_p)$, where $\eta_p \simeq 1.18$ (0.34) for $d = 2$ (3).

Besides the discs and spheres considered here, the percolation of cylinders or ellipsoids will turn out to be of interest to us. While the critical behaviour at the percolation

threshold is universal, i.e., dependent only on the space dimension of the problem, the threshold value itself is affected by the geometry of the objects distributed in space. For ellipsoids, percolation has been studied numerically in considerable detail [13]: as representative illustration, the threshold density for percolation is found to be

$$n_p \simeq \frac{0.21}{(4\pi/3)ab^2}, \quad (10)$$

in the case of an aspect ratio $a/b = 4$ (a is the long, b the short axis of a prolate ellipsoid).

In section 3, we had noted the Coniglio-Klein cluster definition [7], which resulted in the coincidence of percolation and thermal critical behaviour of the Ising model. For our later considerations, the extension of this definition to the continuum is necessary. This, however, for the moment appears to remain an interesting open problem in percolation theory [14].

5. Percolation in QCD

We now turn to the application of percolation in the study of strongly interacting matter and consider first pure colour $SU(N)$ gauge theory. Here the problem is straightforward: we have to extend the Coniglio-Klein approach [7] to continuum percolation, i. e., construct a cluster definition which moves the critical behaviour at the percolation threshold from the universality class of geometric percolation to that of thermal critical behaviour of a Z_N spin system [15]. If this is possible, glueball percolation will lead to the correct deconfinement behaviour as obtained in terms of the Polyakov loop as order parameter.

For the case of QCD with dynamical quarks, it had already been noted in the first studies [1, 2] that the percolation of spheres of hadronic size cannot mean deconfinement: using Eq. (9) and a hadron radius $r = 1.0$ fm, the percolation threshold becomes $n_p \simeq 0.08$ fm⁻³, i.e., it lies below normal nuclear density. Hence at this density, the quarks must still remain effectively localized in colour singlet states, so that the percolation point here corresponds to the formation of connected nuclear matter. Deconfinement, it was argued, occurs only when percolation sets in for some smaller ‘hard core’ of hadrons. The question was how to define this.

In QCD, two fundamental triplet charges are connected by a colour flux tube or string, with $\sigma \simeq 0.16$ GeV² as string tension. The transverse radius r of these strings has the form [16, 17]

$$r^2 = \frac{1}{\pi\sigma} \ln(l/l_0), \quad (11)$$

where $l_0 \simeq 0.1 - 0.3$ fm is the string formation length [18, 19]. Extensive lattice QCD studies find that in the range $0.5 \leq l \leq 2$ fm, $r \simeq 0.2 - 0.3$ fm and varies at most weakly [17, 19]. As a result, a hadron appears as a cylindrical string of diameter $2r$ and length $l \simeq 1$ fm, oscillating about its center of mass to fill a sphere of that radius. While the energy density in the string of length l and radius r is of order 5 GeV/fm³, the oscillation spreads this over a sphere of radius l and thus reduces the energy density to the 0.2 - 0.3 GeV/fm³ observed for a normal (non-Goldstone) meson.

Given such a partonic substructure of a hadron, it becomes clear that deconfinement requires the percolation of the underlying strings. Evidently (compare Eqs. (9) and (10)) this leads to a much higher percolation threshold: while spheres of radius $r = 1$ fm percolate at $n_p^{\text{sphere}} \simeq 0.08 \text{ fm}^{-3}$, the threshold for strings of that length and of radius 0.25 fm (taken as corresponding ellipsoids) becomes more than ten times higher, with $n_p^{\text{string}} \simeq 1.06 \text{ fm}^{-3}$. For (non-Goldstone) hadrons having a generic mass of about 1 GeV, this leads to deconfinement at an energy density around 1 GeV/fm^3 , in general agreement with lattice results. Equating Eqs. (9) and (10) gives

$$r^{\text{core}} \simeq 0.46 \text{ fm} \quad (12)$$

as the radius for the percolation of spheres equivalent to the given string percolation. The ‘hard core’ needed to define deconfinement thus has a radius of about half that of a hadron.

Once the problem of extending the Coniglio-Klein cluster definition to the continuum is solved, we can propose to identify the onset of deconfinement with the percolation threshold for strings of radius r and hadronic length l . In the limit of infinite quark mass, the critical behaviour of $SU(N)$ gauge theory and the corresponding percolation then coincide by virtue of the Coniglio-Klein construction. For any finite value of the bare quark mass, the QCD counterpart of the Kertész line will separate a high density colour conducting deconfined region – the percolation regime – from a low density confined colour insulator, the finite cluster regime. In the confined region, the average Polyakov loop does not vanish; it is only exponentially small, $L \sim \exp(-M_h/T)$, because of occasional thermal string breaking. On the other hand, the average cluster size in this region is finite, so that the percolation probability remains zero up to the percolation threshold.

6. Deconfinement in Nuclear Collisions

While deconfinement in an equilibrated QCD medium thus should start at the percolation threshold for a system of randomly oriented strings, the pre-equilibrium situation encountered in nuclear collisions provides an alignment or polarization of these strings. Consider a central high energy collision of two identical heavy nuclei, in which essentially all nucleons undergo several interactions. These occur in such rapid succession that the nucleons cannot ‘recover’ before being hit again. Each individual nucleon-nucleon collision establishes a colour flux tube or string between the collision partners; the additive quark model [20] suggests that at present (SPS) energies it connects two triplet colour charges, so that it is just the string considered above [16, 17]. For nuclear collisions in their early stage, we thus obtain a spaghetti-like structure of intertwined, overlapping QCD strings, and a cut in the transverse plane results in the picture shown in Fig. 5, giving a distribution of transverse string areas over a circle of nuclear area. Hence the two-dimensional continuum percolation theory presented above is the tool to study what happens when these strings overlap more and more to form connected spatial regions of increasing size in the transverse plane². One important modification is that the overall size of the transverse area is now fixed by nuclear dimensions, requiring the study of finite size cluster formation.

²The first study of this kind was carried out in a specific phenomenological string model [21].

We first consider the cluster density in the transverse plane, then the geometric cluster size as function of the density of the overall density of string discs. To have a specific case, we set $R/r = 20$, corresponding to $R = 5$ fm and $r = 0.25$ fm; to eliminate some of the dependence on the specific choice of parameters, it is convenient to make all quantities (n , n_{cl} and s_{cl}) dimensionless by defining them in terms of πr^2 . In Fig. 6 the resulting cluster density n_{cl} is seen to increase monotonically with the overall density n . As expected from percolation theory, the size s_{cl} of the cluster, in contrast to its density, shows a dramatic variation with n . As noted in section 4, s_{cl} diverges for $R/r \rightarrow \infty$ at the percolation point $n_p = 1.175$, i.e., when the overall density is somewhat above one disc per disc area. Of course there is a considerable overlap of discs, and at n_p , the ratio of the area covered by discs to the overall area becomes $1 - \exp[-1.12] \simeq 0.67$; it approaches unity only for $n \rightarrow \infty$. For finite R/r , the critical behaviour is softened by finite size effects, and for the value $R/r = 20$ chosen above, we obtain the cluster size behaviour shown in Fig. 7. It indeed shows the strongest variation around the percolation point.

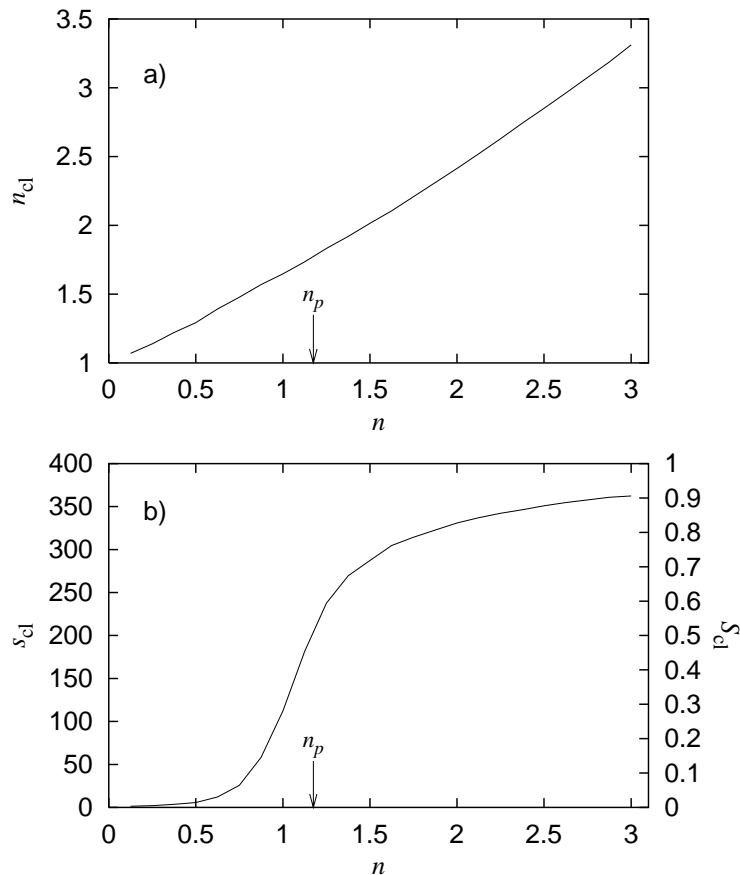


Figure 6: Cluster density (a) and cluster size (b) as function of overall density, in two dimensions, with $r = 0.25$ fm, $R = 5$ fm; n_p denotes the infinite area percolation point.

Deconfinement is expected to set in when there is enough ‘internetting’ between interacting nucleons [23], i.e., when the collision density within a cluster becomes sufficiently

high; we denote this value by n_{cl}^c . It is reached at a certain value $n_c = n(n_{\text{cl}}^c)$ of the overall density, which can, but does not need to be the ultimate percolation point. By Fig. 7, this identifies a corresponding critical cluster size $s_{\text{cl}}^c = s_{\text{cl}}(n_{\text{cl}}^c)$. In other words, requiring a critical collision density automatically forces the cluster to have a certain minimum size. This result answers the question of how much medium is needed before one can speak about a new phase: systems of geometric size $s_{\text{cl}} < s_{\text{cl}}^c$ will on the average not have a string density sufficient for deconfinement.

The onset of deconfinement in nuclear collisions is thus governed by two parameters: the deconfinement string density n_{cl}^c (which could be the percolation value) and the transverse string size r (which is roughly determined by QCD [16, 17]). The size of the nuclear transverse area πR^2 is determined by nuclear geometry. With n_{cl}^c and r fixed, we can then determine the size s_{cl}^c of the bubbles of deconfined medium present at the deconfinement threshold. Realistic nuclear distributions [22] and a Glauber-based formalism must be used to calculate the distribution of collisions in the transverse plane as function of the impact parameter in $A - B$ collisions [23]. The distribution of the strings in the transverse plane is then no longer random, but governed by the nucleon-nucleon collision density thus determined. The resulting formalism can be used to study the onset of deconfinement, using the predicted J/ψ suppression as indicative signal [24]. Here the finite cluster size at the deconfinement threshold leads to an abrupt onset of such suppression [25], which agrees well with the recently reported anomalous J/ψ suppression in $Pb - Pb$ collisions at the CERN-SPS [26]. Moreover, the critical density n_c needed here also agrees rather well with the (infinite volume) percolation point.

Acknowledgements

It is a pleasure to thank Ph. Blanchard, F. Karsch, M. Nardi and D. Stauffer for helpful comments and discussions.

References

- [1] G. Baym, *Physica* 96A (1979) 131.
- [2] T. Çelik, F. Karsch and H. Satz, *Phys. Lett.* 97B (1980) 128.
- [3] For a recent survey, see D. Stauffer and A. Aharony, *Introduction to Percolation Theory*, Taylor & Francis, London 1994.
- [4] P. Hasenfratz, F. Karsch and I. O. Stamatescu, *Phys. Lett.* 133 B (1983) 221.
- [5] R. Pisarski and F. Wilczek, *Phys. Rev.* D29 (1984) 339.
- [6] For surveys, see e. g.
M. B. Isichenko, *Rev. Mod. Phys.* 64 (1992) 961;
C. D. Lorenz and R. M. Ziff, *Phys. Rev.* E 57 (1998) 230.

- [7] A. Coniglio and W. Klein, J. Phys. A 13 (1980) 2775.
- [8] J. Kertész, Physica A 161 (1989) 58.
- [9] R. H. Swendsen and J.-S. Wang, Phys. Rev. Lett. 58 (1987) 86.
- [10] T. D. Lee and C. N. Yang, Phys. Rev. 87 (1952) 404.
- [11] J. Adler and D. Stauffer, Physica A 175 (1991) 222.
- [12] U. Alon, A. Drory and I. Balberg, Phys. Rev. A 42 (1990) 4634.
- [13] E. J. Garboczi, K. A. Snyder, J. F. Douglas and M. F. Thorpe, Phys. Rev. E 52 (1995) 819.
- [14] A. Coniglio, private communication.
- [15] B. Svetitsky and L. G. Yaffe, Nucl. Phys. B 210 [FS6] (1982) 423.
- [16] M. Lüscher, G. Münster and P. Weisz, Nucl. Phys. B 180 (1981) 1.
- [17] For a survey, see E. Laermann, in *QCD - 20 Years Later*, P. Zerwas and H. Kastrup (Eds.), World Scientific, Singapore 1993.
- [18] O. Alvarez, Phys. Rev. D24 (1981) 440.
- [19] For recent precision studies, see G. Bali, K. Schilling and C. Schlichter, Phys. Rev. 51 (1995) 5165 and Nucl. Phys. B (Proc. Supp.) 42 (1995) 273.
- [20] E. M. Levin and L. L. Frankfurt, JETP Lett. 2 (1965) 65;
H. J. Lipkin and F. Scheck, Phys. Rev. Lett. 16 (1966) 71;
H. Satz, Phys. Lett. 25B (1967) 220.
- [21] N. Armesto, M. A. Braun, E. G. Ferreira and C. Pajares, Phys. Rev. Lett. 77 (1996) 3736.
- [22] C. W. deJager, H. deVries and C. deVries, Atomic Data and Nuclear Data Tables 14 (1974) 485.
- [23] D. Kharzeev, C. Lourenço, M. Nardi and H. Satz, Z. Phys. C 74 (1997) 307.
- [24] T. Matsui and H. Satz, Phys. Lett. 178B (1986) 416.
- [25] M. Nardi and H. Satz, ‘String Clustering and J/ψ Suppression’, Bielefeld Preprint BI-TP 98/10 and hep-ph/9805247.
- [26] L. Ramello (NA50), in *Proceedings of Quark Matter '97*, Tsukuba/Japan, to appear in Nucl. Phys. A.